HHS Public Access

Author manuscript

Vision Res. Author manuscript; available in PMC 2021 December 01.

Published in final edited form as:

Vision Res. 2020 December ; 177: 32–40. doi:10.1016/j.visres.2020.08.003.

Eccentricity-Dependent Effects of Simultaneous Competing Defocus on Emmetropizzation in Infant Rhesus Monkeys

Earl L Smith III[1,2], **Baskar Arumugam**[1,3], **Li-Fang Hung**[1,2], **Zhihui She**[1], **Krista Beach**[1], **Padmaja Sankaridurg**[2,4]

[1]College of Optometry, University of Houston, Houston, Texas, United States

[2]Brien Holden Vision Institute, Sydney, Australia

[3]Former Employee of University of Houston, Houston, Texas, United States

[4]Department of Optometry and Vision Science, University of New South Wales, Kensington, New South Wales Australia

Abstract

Dual-focus lenses that impose simultaneous competing myopic defocus over the entire visual field produce axial hyperopic shifts in refractive error. The purpose of this study was to characterize the effects of eccentricity on the ability of myopic defocus signals to influence central refractive development in infant monkeys. From 24 to 152 days of age, rhesus monkeys were reared with binocular, dual-focus lenses that had central, zero-powered zones surrounded by alternating concentric annular power zones of +3D and zero power. Between subject groups the diameter of the central, zero-powered zone was varied from 2mm to 8mm in 2mm steps (+3D/pl 2mm, n=6; +3D/pl 4mm, n=6; +3D/pl 6mm, n=8, or +3D/pl 8mm, n=6). For the treatment lens with 2, 4, 6 and 8 mm central zones, objects at eccentricities beyond 11°, 16°, 19° and 23°, respectively, were imaged exclusively through the dual-power peripheral zones. Refractive status (retinoscopy),

Corresponding author: Earl L. Smith III, University of Houston, College of Optometry, 4901 Calhoun Road, 505 J Armistead Building, Houston, TX 77204-2020, Tel: 713-743-1946; Fax: 713-743-2053; esmith@uh.edu.

Earl L Smith III
Conceptualization, Methodology, Formal analysis, Investigation, Resources, Writing – original and review, Visualization, Supervision, Project Administration, Funding Acquisition, Validation

Baskar Arumugam
Conceptualization, Methodology, Formal analysis, Investigation, Writing – review & editing

Li-Fang Flung
Conceptualization, Methodology, Formal analysis, Investigation, Writing – review & editing, Data Curation

Zhihui She
Methodology, Formal analysis, Investigation, Writing – review & editing

Krista Beach
Methodology, Formal analysis, Investigation, Writing – review & editing

Padmaja Sankaridurg
Writing – review & editing, Project Administration, Funding Acquisition

Declarations of interest

E.L. Smith III, (p) patents on optical and pharmaceutical treatment strategies for myopia, (C) consultant to Nevakar, SightGlass Vision, Treehouse Eyes, Acucela Inc. and Essilor of America; B. Arumugam, None; L.-F. Hung, None; Z. She, None; K. Beach, None; P. Sankaridudrg, (p) patents on optical and pharmaceutical treatment strategies for myopia.

corneal power (keratometry) and axial dimensions (ultrasonography) were measured at two-week intervals. Comparison data were obtained from monkeys reared with binocular, single-vision +3D full-field lenses (+3D FF, n=6) and 41 normal control monkeys reared with unrestricted vision. At the end of the rearing period, with the exception of the +3D/pl 8mm group (median = +3.64 D), the ametropias for the other lens-reared groups (medians: FF=+4.39 D, 2mm=+5.19 D, 4mm= +5.59 D, 6mm=+3.50 D) were significantly more hyperopic than that for the normal monkeys (+2.50 D). These hyperopic errors were associated with shallower vitreous chambers. The key finding was that the extent and consistency of these hyperopic ametropias varied with the eccentricity of the dual-focus zones. The results confirm that myopic defocus in the near periphery can slow axial growth, but that imposed defocus beyond about 20° from the fovea does not consistently alter central refractive development.

Keywords

myopia; emmetropization; animal model; periphery; hyperopia; multifocal lenses; eccentricity

1. Introduction

Myopia is a significant public health concern primarily because structural changes associated with excessive axial elongation put the myopic eye at risk for a number of potentially blinding conditions (Wong, Ferreira, Hughes, Carter & Mitchel, 2014). Given the projected increases in the prevalence and degree of myopia (Holden, Fricke, Wilson, Jong, Naidoo, Sankaridurg, Wong, Naduvilath & Resnikoff, 2016), the burden of myopia on individuals and society is likely to increase in the future, particularly because the ocular morbidity associated with myopia increases with the degree of myopia (Flitcroft, 2012). In this regard, substantial efforts have been and are being devoted to developing treatment strategies that can prevent or reduce the progression of myopia commonly observed in children (Wildsoet, Chia, Cho, Guggenheim, Polling, Read, Sankaridurg, Saw, Trier, Walline, Wu & Wolffsohn, 2019). These efforts are based on the premise that reducing the degree of myopia would have long-term health benefits for patients (Bullimore & Brennan, 2019).

A large body of research involving laboratory animals has provided the scientific motivation for a range of treatment strategies for myopia (Troilo, Smith, Nickla, Ashby, Tkatchenko, Ostrin, Gawne, Pardue, Summers, Kee, Schroedl, Wahl & Jones, 2019). In particular, the finding that optically imposed changes in the eye’s effective refractive status can predictably alter ocular growth and refractive development has provided insights into the genesis of myopia and the rationale for many current optical treatment strategies (Schaeffel, Glasser & Howland, 1988). Specifically, the observation that imposed myopic defocus can slow axial elongation and produce relative hyperopic shifts in a diverse range of laboratory animals (Barathi, Boopathi, Yap & Beuerman, 2008, Howlett & McFadden, 2009, Hung, Crawford & Smith III, 1995, Irving, Callender & Sivak, 1995, Norton & Siegwart, 1995, Whatham & Judge, 2001)(for a review see Troilo et al, 2019) has been the driving force for incorporating optical features into both spectacle and contact lens strategies that correct myopia along the visual axis and simultaneously impose relative myopic defocus (Smith III, 2011, Wildsoet et

al., 2019). Many of these treatment strategies take advantage of three key operating characteristics of the vision-dependent mechanisms that regulate eye growth. First, visual signals that originate in the fovea are not essential for many vision-dependent aspects of ocular growth (Smith III, Kee, Ramamirtham, Qiao-Grider & Hung, 2005, Smith III, Ramamirtham, Qiao-Grider, Hung, Huang, Kee, Coats & Paysee, 2007). Second, signals that originate in the periphery, which are presumably summed over a large proportion of the total retinal area (Wallman & Winawer, 2004), have a substantial effect on axial elongation and refractive development for the "central" macular area of the retina (Benavente-Perez, Nour & Troilo, 2014, Bowrey, Zeng, Tse, Leotta, Wu, To, Wildsoet & McFadden, 2017, Liu & Wildsoet, 2011, Liu & Wildsoet, 2012, Smith III, Hung & Huang, 2009, Smith III, Hung, Huang & Arumugam, 2013, Smith III et al., 2005). And third, when the eye experiences simultaneous competing defocus signals, refractive development is typically directed toward the more anterior focal plane (Arumugam, Hung, To, Holden & Smith III, 2014, Arumugam, Hung, To, Sankaridurg & Smith III, 2016, Benavente-Perez, Nour & Troilo, 2012, McFadden, Tse, Bowrey, Leotta, Lam, Wildsoet & To, 2014, Tse, Lam, Guggenheim, Lam, Li, Liu & To, 2007).

Recent clinical trials have shown that a variety of lens designs that correct distance vision while simultaneously imposing relative myopic defocus over a large part of the retina can reduce myopia progression in children in a clinically meaningful manner (Sankaridurg, 2017, Wildsoet et al., 2019). Understanding how these simultaneous, but competing visual signals, are integrated across the retina is important for optimizing optical treatment strategies. In this regard, the relative effectiveness of these different optical treatment strategies to slow myopia progression appears to reflect the areal extent of the retina that receives relative myopic defocus (Smith III, 2013).

With respect to the contribution of visual signals across the retina to central refractive development, it seems reasonable to assume that signals from the near periphery would have a greater effect on central refractive development than signals from the more peripheral parts of the retina. In other words, the relative weight of signals associated with a given area of retina would decrease with eccentricity, possibly reflecting a reduction in the density of certain retinal neurons. However, these eccentricity-dependent effects would be counterbalanced by the fact that with increasing eccentricity, signals could potentially be summed over a larger proportion of the total retinal area (Wallman & Winawer, 2004). In this regard, knowledge of these relative weighting functions, i.e., how the contributions from a given area of retina to central refractive development vary with eccentricity, is important for optimizing optical treatment regimens. Therefore, the purpose of this study was to investigate the effects of retinal eccentricity on the ability of simultaneously imposed myopic defocus to influence axial elongation and refractive development in the central retinas of infant monkeys.

2. Methods

2.1 Subjects and lens-rearing procedures

The primary subjects were 26 rhesus monkeys (*Macaca mulatta*) that were obtained at 2-3 weeks of age. Beginning at 24 ± 2 days of age the animals were assigned to one of four lens-

treatment groups and fitted with helmets that held dual-focus lenses in front of both eyes. All of the treatment lenses had central zones of zero power (i.e., plano power) that were surrounded by alternating concentric annular power zones of +3 diopters (D) and plano power (+3D/pl dual-focus lenses). The alternating concentric annular power zones had equal 0.4 mm widths. The only between-group difference in the treatment lenses was the diameter of the central zero-power zone, which was varied from 2 to 8 mm in 2 mm steps (+3D/pl 2mm, n = 6; +3D/pl 4mm, n = 6; +3D/pl 6mm, n = 8; and +3D/pl 8mm, n = 6). Note that much of the data for the monkeys in the +3D/pl 2mm group have been previously published (Arumugam et al., 2014).

The treatment lenses, which were similar to the dual-focus lenses employed by Tse et al. (Tse et al., 2007) and manufactured by the State Key Laboratory of Ultra-precision Machining Technology (The Hong Kong Polytechnic University, Hong Kong), had optical zone diameters of 22 mm (central plano zone plus the surrounding dual-focus zones) and were secured by the helmets at a vertex distance of 11 mm centered on each eye's entrance pupil, providing total monocular fields of view of approximately 85°. The schematic diagram in Figure 1 illustrates the extent of the visual field affected by the central plano zones and the dual-focus surrounds of the treatment lenses. We employed the paraxial ray tracing strategies described by Carkeet (Carkeet, 1998) and illustrated in the Supplementary material to determine the visual field locations affected by the central and peripheral power zones and to assess the effects of a number of subject and lens parameters on the field of view through the lenses. In particular, the extent of the visual field influenced by the treatment lens surrounds was dependent primarily on the central zero-power zone diameter and to a smaller degree the size of the eye's entrance pupil and the vertex distance of the lens. Assuming an entrance pupil diameter of 3.3 mm, an anterior chamber depth of 2.58 mm, a corneal power of 61.61 D, the resulting fields of view through the 4, 6, and 8 mm central plano zone diameters were ±1.5°, ±5.8° and ±9.8°, respectively (dotted blue lines in Fig 1). These central zones delineate the object eccentricities that were imaged exclusively through the zero-power zones, i.e., all the rays for these object locations were unaffected by the dual-focus surrounds. With the +3D/pl 2mm lenses, the central zero-power zones were smaller than the pupil diameters of the infant monkeys and, thus, the peripheral power zones affected objects across the entire visual field (i.e., no object locations were imaged exclusively through the 2mm central zones). For object positions outside the dashed red lines, all the rays that contributed to their retinal images passed through the dual-focus surrounds of the treatment lens; and these objects were imaged at two focal planes formed by approximately equal amounts of light. The angular limits of the peripheral zones that produced images from light that passed exclusively through the dual-powered portions of the treatment lenses were ±11.4°, ±15.5°, ±19.4° and ±23.2° for the 2-mm, 4-mm, 6-mm and 8-mm +3D/pl lenses, respectively (dashed red lines in Fig 1). The images of objects located between the dotted and dashed lines in a given hemi-field were also imaged at two focal planes (the variable saliency region in Figure 1). However, the amount of light that contributed to each image plane varied with eccentricity. Specifically the amount of light contributing to the image plane corresponding to the +3D/pl surround zones increased systematically with eccentricity while that for the image plane corresponding to the plano central zones decreased with eccentricity (see Supplementary material).

The helmets and treatment lenses were inspected at approximately 2-hour intervals throughout the day to ensure that the helmets fit the subjects appropriately and that the spectacle lenses were free of debris that might have interfered with the desired optical effects. Except for the brief periods needed for routine cleaning, the lenses were worn continuously until 152 ± 3 days of age.

We chose to use +3D/pl lenses because this degree of imposed relative spherical myopic defocus consistently produces compensating responses in infant monkeys (Hung et al., 1995, Smith III & Hung, 1999). Moreover, similar powered dual-focus lenses that produced competing defocus signals across the entire retina consistently produced hyperopic shifts in young monkeys toward the more anterior focal plane (Arumugam et al., 2014). In many respects, the competing defocus signals produced by the +3D/pl lenses were analogous to the optical effects associated with many optical treatment strategies that are currently being used to manage myopia progression in children (i.e., a distance correction paired with a +3 D add). In addition, we employed a binocular treatment strategy to more closely mimic the viewing conditions associated with these common clinical treatment regimens.

Throughout the treatment period, we visually assessed the animals viewing behavior multiple times each day by attracting the animals' attention to different objects. We consistently observed that the monkeys would make head movements to fixate novel objects through the central zero-powered zones of the lenses. In particular, when the monkeys fixated an investigator, the monkey's pupils were observed to be in the center of the treatment lens central zones, presumably because viewing through the dual-focus surrounds would degrade their central vision. However, we made no attempts to quantify the monkeys' fixation behavior. In this respect, it is likely that our monkeys intermittently fixated through the periphery of the dual-focus lenses, for example during convergence on very near targets or if they made large eye movements.

Control data were available for 41 normal monkeys reared with unrestricted vision (34 animals from previous studies and 7 monkeys studied following the onset of the dual-focus lens experiments) and 6 monkeys reared with binocular full-field, single-vision +3D lenses (+3D FF group) (Arumugam et al., 2014, Arumugam et al., 2016, Smith III & Hung, 1999). Although the data for the control animals, particularly the animals reared with unrestricted vision, were collected over a period of years, the husbandry, the general lens-rearing protocols, and the biometric measurement methods were similar in every respect to those employed in this study with the animals reared with dual-focus lenses.

Throughout the observation period, the housing areas for all of the treated and control animals were illuminated with "white" fluorescent lights (GE Ecolux® Starcoat® T8 F32T8/SP35/ECO, General Electric Co., Boston, MA) on a 12-hr light / 12-hr dark cycle with the light onset occurring at 7:00 am. The cage level illuminance varied between 350 to 504 lux (Spectrophotometer CL-500A, Konica Minolta Sensing America, Inc. Ramsey, NJ, USA).

2.2 Ocular Biometry

The animals' refractive status, central corneal powers, and axial dimensions were assessed at the onset of lens wear and subsequently at approximately 2-week intervals throughout the lens-rearing period. To make these measurements the monkeys were anesthetized with an intramuscular injection of ketamine hydrochloride (15-20 mg/kg) and acepromazine maleate (0.15-0.2 mg/kg) and the topical instillation of 0.5% tetracaine hydrochloride. Cycloplegia was induced by the instillation of 1% tropicamide 25 and 20 minutes before any measures that would be affected by pupil size or accommodation. The refractive state of each eye along its pupillary axis was measured independently by two experienced investigators using a streak retinoscope, averaged (Harris, 1988, Kee, Hung, Qiao-Grider, Roorda & Smith III, 2004), and specified as the spherical-equivalent, spectacle-plane refractive correction. The central cornea's anterior radius of curvature was measured using a hand-held keratometer (Alcon Auto-keratometer; Alcon, Inc., St. Louis, MO) or a EyeSys 2000 video topographer (EyeSys Vision, Inc. Houston, TX) when the corneal power exceed the measurement range of the keratometer (i.e., >+62 D; approximately 5% of 3-week-old monkeys). Three radius of curvature readings obtained with the keratometer were averaged and the central corneal power was calculated assuming that the cornea was a single spherical refracting surface and using an assumed index of refraction for image space of 1.3375 (Kee, Hung, Qiao & Smith III, 2003). Axial ocular dimensions were measured by A-scan ultrasonography using a direct contact 13-MHz transducer (Image 2000, Mentor, Norwell, MA, USA). Ten reading were averaged to obtain the dimensions for the anterior chamber, lens thickness and vitreous chamber depth (Smith III, Hung & Huang, 2012).

The rearing and experimental procedures were approved by the University of Houston's Institutional Animal Care and Use Committee and were in compliance with the ARVO Animal Statement and the National Institutes of Health Guide for the Care and Use of Laboratory Animals.

2.3 Statistical Methods

Statistical analyses were performed using Minitab (Release 16.2.4, Minitab Inc., State College, PA) and Super ANOVA software (Abacus Concepts, Inc., Berkeley, CA). Because the distribution of refractive errors in normal monkeys at ages corresponding to the end of the treatment period is leptokurtic, nonparametric Mann-Whitney tests were used to compare the end-of-treatment refractive errors between the treated and normal control groups and medians were employed as measures of central tendency. For all other between group comparisons, the data were normally distributed and averages (arithmetic "means") were used as measures of central tendency and student T tests were used for between group comparisons. With two exceptions, standard deviations (SD) were employed to characterize the dispersion of data from the mean. However, to improve visibility in Figures 3A and 6, the error bars represent standard errors of the mean (SEM), Paired-student T-tests were employed to examine the interocular differences in ocular parameters within a given subject group. Mixed-design ANOVAs with Greenhouse-Geisser (G-G) corrections for multiple testing were used to compare between groups the changes in refractive error and vitreous chamber depth that occurred during the observation period. The relationship between refractive error and the ratio between vitreous chamber depth and anterior corneal radius was

characterized using linear regression analyses. As detailed below, there were no systematic interocular differences in refractive error or ocular dimensions for monkeys in any subject group. Therefore, the refractive error and ocular parameters for a given monkeys were defined as the average values for their left and right eyes.

3. Results

At baseline the animals assigned to the lens-treatment groups exhibited moderate degrees of hyperopia that were statistically comparable to those found in the normal control monkeys (averages ± SD: control monkeys = +3.81 ± 1.73 D; +3D FF = +4.15 ± 1.56 D, T = 0.48, P = 0.65, df = 6; +3D/pl 2mm = +4.10 ± 1.22 D, T = 0.51, P = 0.72, df = 8; +3D/pl 4mm = 4.26 ± 1.20 D, T = 0.80, P = 0.46, df = 8; +3D/pl 6mm = +3.63 ± 0.50 D, T = 0.58. P = 0.72, df = 39; +3D/pl 8mm = +2.95 ± 1.12 D, T = 1.63. P = 0.14, df = 9). There were also no between group differences in corneal power (T = 0.83 to 0.99, P > 0.26 to 0.99, df = 7 to 13), and with the exception of the +3D/pl 2 mm treatment group, which had, on average, shallower vitreous chambers than normal controls (8.42 ± 0.14 mm vs 8.61 ± 0.31 mm; T = 0.28, P = 0.02, df = 12), there were no between group differences in ocular axial dimensions. Moreover, the two eyes of individual animals were well-matched. At the start of the lens-rearing period, there were no significant interocular differences in refractive error (T = 0 to 1.74. P = 0.13 to 1.0) or corneal power (T = 0.07 to 1.96. P = 0.12 to 0.95). Again with the exception of the animals in the +3D/pl 2mm group that showed a statistically significant, but not very meaningful, interocular difference in vitreous chamber depth (8.41 ± 0.14 mm vs 8.43 ± 0.15 mm; T = −3.73, P = 0.01), there were no systematic interocular differences in ocular axial dimensions in either the treated or control groups.

In Figure 2, the refractive errors measured during the lens-rearing period are plotted as a function of age for individual animals in each treatment group. Because there were no systematic interocular differences in refractive error during or at the end of the treatment period, each of the smaller data points represents the mean refraction derived from results for the left and right eyes of a given animal. The shaded area in each plot represents the 10% to 90% limits for the range of refractive errors in the normal control animals.

At the onset of lens wear (the first data point for each function), 29 of the 32 lens-treated monkeys had initial refractive errors that fell within the 10% to 90% limits for normal monkeys. Imposing 3 D of relative myopic defocus across the entire visual field consistently altered the target refractive error for emmetropization. All of the infants that were treated with +3D FF (full-field) lenses either maintained their moderate hyperopic errors throughout the treatment period or exhibited hyperopic shifts in refractions (Figure 2A). As a result, at the end of the treatment period all 6 of the monkeys in the +3D FF group exhibited ametropias that were more hyperopic than 90% of the normal control monkeys. The +3D/pl dual-focus lenses also altered the course of emmetropization; however, the extent and consistency of these alterations varied with the diameter of the central plano-power zone. All of the animals in both the +3D/pl 2mm (panel 2B) and +3D/pl 4mm treatment groups (panel 2C) demonstrated relative hyperopic shifts during the lens-rearing period, and their final refractive errors were well outside the 90% limits for normal monkeys. The effects of the dual-focus lenses with 6 mm (panel 2D) and 8 mm central plano zones (panel 2E) were

much less consistent, as reflected by the standard deviations of the end-of-treatment average refractive errors (large circles with error bars to the right in each plot). While 5 of the 8 monkeys in the +3D/pl 6mm group and 3 of the 6 animals in the +3D/pl 8mm group developed hyperopic errors that were above the 90% limits for normal monkeys, 2 monkeys in each of these groups exhibited refractive errors within the 10% to 90% normal limits and 1 monkey in each group exhibited systematic reductions in hyperopia early in the treatment period that stabilized at ametropias that were less hyperopic than 90% of the normal monkeys.

Figure 3A compares the average (±SEM) changes in refractive error that were observed in each of the subject groups relative to their baseline ametropias. The normal control monkeys typically exhibited relative reductions in hyperopia associated with emmetropization. On the other hand, the lens-reared monkeys on average demonstrated little or no changes in refractive error (e.g., the animals reared with +3D FF lenses and dual-focus lenses with 6mm or 8mm central plano zones) or systematic increases in hyperopia during the treatment period (e.g., the monkeys reared with the +3D/pl 2mm and 4 mm treatment lenses). The longitudinal changes in refractive error for all of the lens-reared animals were significantly less myopic/more hyperopic than those observed in normal monkeys (a mixed-design ANOVA ;+3D/pl FF, $F = 7.69$, $P = 0.0007$, df = 9; +3D/pl 2mm, $F = 12.34$, $P = 0.0001$, df = 9; +3D/pl 4mm, $F = 17.29$, $P = 0.0001$, df = 9; +3D/pl 6mm, $F = 6.53$, $P = 0.003$, df = 9; +3D/pl 8mm, $F = 4.24$, $P = 0.02$, df = 9). In addition, the magnitude of the refractive-error changes exhibited over the course of the treatment period by the animals in the +3D/pl 4mm group (+1.57 ± 0.79 D) were more hyperopic than those observed in the FF (+0.19 ± 1.29 D; $T = 2.23$, $P = 0.03$, df = 8), 2 mm (+0.82 ± 0.59 D; $T = 1.85$. $P = 0.05$, df = 9) 6 mm (+0.22 ± 1.63 D; $T = 2.04$, $P = 0.04$, df = 10) or 8 mm treated subject groups (+0.26 ± 1.58 D; $T = 1.81$, $P = 0.057$, df = 7).

These lens-induced alterations in the course of emmetropization resulted in higher than normal degrees of hyperopia, as illustrated by the box plots of the end-of-treatment ametropias in Figure 3B. With the exception of the +3D/pl 8mm group (median = +3.64 D, Mann-Whitney, $P = 0.10$), the ametropias for all of the other lens-reared groups (medians: FF = +4.39 D, $P < 0.001$; 2mm = +5.19 D, $P < 0.001$; 4mm = +5.59 D, $P < 0.001$; 6mm = +3.50 D, $P = 0.006$) were significantly more hyperopic than that for the normal control monkeys (+2.50 D). The final average refractive error for the +3D/pl 4mm group (see Table 1), which was consistently the most hyperopic of the lens-reared groups (+5.83 ± 0.67 D), was similar to that for the +3D/pl 2mm subjects (+5.08 ± 0.94 D, $T = 1.56$, $P = 0.08$, df = 8), but significantly more hyperopic than those for the monkeys reared with the +3D FF lenses (+4.34 ± 0.88 D, $T = 3.28$. $P = 0.005$, df = 9) and the dual-focus lenses with 6mm (+3.85 ± 1.70 D, $T = 3.0$, $P = 0.007$, df = 9) and 8mm central plano power zones (+3.31 ± 1.54 D, $T = 3.81$, $P = 0.004$. df = 6).

The refractive-error alterations produced by the treatment lenses were associated with alterations in vitreous chamber elongation rate. The relative changes in vitreous chamber depth that took place during the lens-rearing period are plotted as a function of age for individual treated animals in Figure 4. For comparison purposes, the mean changes in vitreous chamber depth for the normal control monkeys have been included in each panel.

The treatment lenses that consistently resulted in relative hyperopic shifts consistently reduced the rate of vitreous chamber elongation. Five of the 6 animals in the +3D FF, +3D/pl 2mm and +3D/pl 4mm treatment groups (panels A-C) exhibited vitreous chamber elongation rates that were lower than the average normal monkey, and a mixed-design ANOVA showed the overall pattern of vitreous chamber growth during the lens-rearing period was statistically slower in the 2mm (F = 3.70, $P = 0.03$, df = 9) and 4mm dual-focus animals (F = 10.61, $P = 0.0004$, df = 9). However, vitreous chamber elongation in the +3D FF group was not statistically different from that in the control animals (F = 0.96, $P = 0.38$, df = 9), in large part due the contribution of an outlier in the FF group. The +3D/pl 6mm and 8mm lens-reared groups (panels D and E) exhibited substantial between-subject differences in vitreous chamber elongations rates. However, the elongation rates for individual animals corresponded to their changes in refractive error. For example, the monkeys in each of these groups that had the lowest degree of hyperopia at the end of the treatment period exhibited the fastest vitreous chamber elongation rates in their respective group. Similarly, the monkeys in these groups that showed the largest hyperopic shifts during the lens rearing period also exhibited the slowest vitreous chamber elongation rates.

At the end of the treatment period, there were clear between-group differences in absolute vitreous chamber depth (Figure 5A). In comparison to normal monkeys (9.84 ± 0.31 mm), the average vitreous chambers were significantly shallower in the +3D/pl 2mm (9.38 ± 0.35 mm, T = 2.99, $P = 0.02$, df = 6) and +3D/pl 4mm groups (9.40 ± 0.23 mm, T = 4.08, $P = 0.004$, df = 8). Likewise, the vitreous chamber depths in the monkeys that wore treatment lenses with the 2mm and 4mm zero-power zones were significantly shallower than those in the +3D/pl 8mm animals (9.90 ± 0.42, T = −2.30, $P = 0.04$, df = 9). The average vitreous chamber depth for the +3D FF monkeys (9.59 ± 0.32 mm) was more than 0.2 mm shallower than that for the normal monkeys, but this difference was not statistically different (T = 1.72, $P = 0.14$, df = 6)

The average corneal powers, anterior chamber depths, and lens thicknesses obtained at the end of the treatment period for the animals reared with dual-focus lenses were statistically similar to those in the normal control monkeys (see Table 1). However, the anterior chambers of the +3D FF monkeys were significantly shallower (2.90 mm vs 3.09 mm, T = 2.67, $P = 0.02$, df = 13) than those of the normal control monkeys. At baseline, the anterior chambers of the +3D FF monkeys were on average about 0.08 mm shallower than that for the normal monkeys, but this difference was not significant (2.45 ± 0.07 mm versus 2.53 ± 0.16 mm, T = 2.00, P = 0.06, df = 17). We have not observed vision-induced alterations in anterior chamber depth in any previous studies.

Figure 5B, which shows the final refractive errors for each animal plotted as a function of the ratio of vitreous chamber depth in mm to corneal radius in mm, emphasizes the axial nature of the refractive errors in the treated animals. Although there were no systematic differences in corneal power between the control (55.93 ± 1.60 D) and dual-focus animals at the end of the treatment period (+3D/pl 2mm = 55.45 ± 1.00 D, T = 1.03, $P = 0.32$, df = 12; +3D/pl 4mm = 55.39 ± 1.09 D, T = 1.03, $P = 0.33$, df = 8; +3D/pl 6mm = 55.72 ± 1.63 D, T = 0.32, $P = 0.76$, df = 10; +3D/pl 8mm = 55.86 ± 1.75 D, T = −0.09, $P = 0.93$, df = 6), there were inter-subject differences in corneal power within and between subject groups that were

sufficient to partially mask the relationship between refractive error and absolute vitreous chamber depth. Employing the ratio of vitreous chamber depth to corneal radius compensates, at least in part, for the effects of inter-subject differences in absolute corneal power on vitreous chamber depth, thus highlighting the effects of vitreous chamber depth on refractive error. As illustrated in Figure 5B, the vitreous chamber / corneal radius ratio reliably predicts refractive error ($r^2 = 0.68$; $P < 0.0001$).

4. Discussion

In agreement with previous experiments employing dual-focus treatment lenses in infant monkeys (Arumugam et al., 2014, Arumugam et al., 2016), simultaneous competing myopic defocus biased the target refractive error for the emmetropization process toward the more myopic/less hyperopic focal plane. In a similar manner, in monkeys reared with optically imposed astigmatism, which also produces two competing simultaneous image planes, the emmetropization process was found to most frequently target the more anterior focal plane (Kee et al., 2004). These results are in line with a large body of research that has shown that myopic defocus has a stronger effect on refractive development than hyperopic defocus (Troilo et al., 2019, Wallman & Winawer, 2004, Zhu, Winawer & Wallman, 2003). The key findings from this study were that myopic defocus signals in the periphery can dominate central refractive development, but that the ability of simultaneous competing myopic defocus signals to alter central refractive development varied with eccentricity. In particular, competing myopic defocus signals imposed closer to the fovea generally had greater and more consistent effects on slowing axial growth and producing relative hyperopic shifts in the central refraction than myopic defocus imposed at greater eccentricities.

4.1 Eccentricity-Dependent Effects: Comparisons to Other Studies

In a previous experiment, we reared infant monkeys with −3.0 D, single-vision lenses with central apertures (Smith III et al., 2009). These lenses produced unrestricted central vision (approximately the central 10°). However, objects that were located outside the central 31° (i.e., eccentricities >15.5°) were imaged exclusively through the powered portion of the lens. Our main finding was that relative peripheral hyperopic defocus could override the effects of unrestricted central vision and produce central axial myopia. The peripheral optical effects of the dual-focus lenses employed in this study were more complex, producing overlapping competing defocus signals outside the central zones of unrestricted vision. Nevertheless, the results were qualitatively similar. In both cases, when there were conflicting defocus signals in the periphery versus the central retina, the peripheral visual signals could dominate central axial growth and refractive development. In particular, our results show that in macaques myopic defocus imposed in the near periphery can produce central axial hyperopia independent of the nature of central vision.

Qualitatively similar patterns of results have been previously reported for chickens (Liu & Wildsoet, 2011), marmosets (Benavente-Perez et al., 2014) and guinea pigs (Bowrey et al., 2017) that were reared with concentric, bifocal treatment lenses that provided unrestricted central vision and that imposed relative myopic defocus in the periphery. Specifically, in each species peripheral myopic defocus produced relative hyperopic shifts in the refractive

state of the central retina, typically by reducing axial elongation. In addition, in both marmosets (Benavente-Perez et al., 2014) and chickens (Liu & Wildsoet, 2011, Liu & Wildsoet, 2012) the ability of relative peripheral myopic defocus to influence central refractive development was greatest when the imposed myopic defocus was closer to the central retina (see Figure 6).

In Figure 6, the effects of imposed peripheral defocus are plotted as a function of the eccentricity of the exclusive peripheral defocus zones for both monkeys and chickens. The effects are expressed relative to the alterations in central refractive error produced by full-field, single-vision lenses that had dioptric powers equivalent to the relative degrees of imposed peripheral defocus (3.0 D for monkeys; 5.0 D or 7.0 D for chickens). For the dual-focus monkeys (blue squares), the vertical error bars represent ±1 SEM; the horizontal error bars represent the combined uncertainty of the eccentricity values associated with ±1 mm change in vertex distance together with a ±0.6 mm change in pupil size (i.e., a change in pupil size equivalent to 2 SDs of the average pupil size). An interesting feature of the data is that for both monkeys and chickens, imposing myopic defocus in the periphery can produce larger alterations in central refractive error than a similar degree of myopic defocus imposed across the entire retina. Similarly, in marmosets, concentric bifocals with small central zones of unrestricted vision that imposed relative peripheral myopia produced changes in central refractive error that were larger and lasted longer than those produced by positive-powered, single-vision lenses (Benavente-Perez et al., 2014).

What is responsible for the enhanced treatment effects when relative myopic defocus is imposed in the near periphery (as observed for the +3D/pl 4mm lens group)? It is possible that the enhanced treatment effects come about because high-order aberrations, particularly spherical aberration, concomitantly induced by concentric, multi-focal treatment lenses interact with the eye's optics to alter the target plane for emmetropization (Liu & Wildsoet, 2011). However, it is likely that the refractive alterations produced by concentric multi-focal lenses are more robust than those produced by single-vision lenses because peripheral defocus signals can dominate central refractive development and the imposed peripheral myopic defocus signals do not necessarily decrease as the central refraction becomes more hyperopic (Schaeffel, 2017). With positive-powered, single-vision lenses, the imposed error signal decreases across the retina as the eye compensates for the imposed defocus. However, that is not necessarily the case with concentric, multi-focal lenses with zero power in the center of the lens and positive peripheral power. Instead as the eye's refraction shifts in the hyperopic direction, the imposed error signal in the periphery would decrease, but the effective central hyperopic error would increase, reducing central vision (assuming that the eye is unaccommodated). In this situation, it is reasonable to suppose that to achieve clear central vision the eye would accommodate to overcome the central hyperopia. This scenario is reasonable because accommodation, although influenced by peripheral retinal signals, is dominated by foveal signals (Hartwig, Charman & Radhakrishnan, 2011, Labhishetty, Cholewiak & Banks, 2019). The resulting positive accommodation, while improving central vision, would re-establish the relative peripheral myopia imposed by peripheral-plus treatment lenses. In agreement with this idea, we previously reported that monkeys accommodated normally for near objects when viewing through +3D/pl 2mm lenses (Arumugam et al., 2014). Thus, the absolute degree of the peripheral error signal would not

necessarily decrease as the central refraction became more hyperopic, at least when the eye was accommodating to compensate for its hyperopic refractive error.

Inspection of Figure 6 also reveals that the absolute range of eccentricities over which imposed optical defocus can influence central refractive development is quite different in monkeys and chickens. In monkeys, although there are obvious inter-animal differences in the responses to dual-focus lenses, myopic defocus imposed at eccentricities up to about 20° can have a strong influence on central refractive development, perhaps reflecting the fact that vision-induced refractive errors are associated with biochemical (and possibly biomechanical) changes that are largely restricted to the posterior sclera in mammals (Norton & Rada, 1995, Rada, Nickla & Troilo, 2000). On the other hand, in chickens imposed defocus was very effective in altering central refractive development even at eccentricities over 40° (Liu & Wildsoet, 2011). There are a variety of methodological issues that are likely to impact the differences noted between chickens and monkeys (e.g., dual-focus peripheral optics versus the mono-focal peripheries of concentric bifocals), however, it is also likely that differences in retinal anatomy and physiology play a role. For example, the macaque retina, like the human retina, is rod-dominated with a highly developed, cone-dominated fovea. Cone density and visual acuity decrease significantly with eccentricity in the primate retina (Rolls & Cowey, 1970). In contrast, the chicken retina is cone dominated and visual acuity appears to be relatively uniform across a large part of the retina (Maier, Howland, Ohlendorf, Wahl & Schaeffel, 2015, Troilo et al., 2019). Perhaps peripheral control signals play a bigger role in chickens because it may be more important to optimize focus across a larger area of retina than in primates

4.2 Implications for optical treatment strategies to slow myopia progression

The results from this study, as well as those from previous studies in chickens (Liu & Wildsoet, 2011, Liu & Wildsoet, 2012, Rolls & Cowey, 1970), marmosets (Benavente-Perez et al., 2014), and guinea pigs (Bowrey et al., 2017), support the idea that treatment strategies that correct central vision and that simultaneously impose relative myopic defocus in the peripheral visual field can be effective in reducing axial elongation and myopia progression in children (Smith III, 2011). In this respect, multiple clinical trials involving a variety of optical treatment strategies that effectively imposed relative myopic defocus over a large part of the peripheral retina have demonstrated clinically meaningful reductions in myopia progression (Sankaridurg, 2017, Wildsoet et al., 2019). However as highlighted in Figure 6, the effective eccentricity and probably the total area of the retina exposed to myopic defocus are likely to affect the efficacy of these optical treatment strategies. Specifically, our results indicate that in order to consistently slow central axial elongation, the imposed myopic defocus should occur within about 20° of the foveal center, with maximal effects taking place when the myopic defocus was imposed within the central 15°.

Comparisons of the results across clinical trials suggest that the relative ability of different lens designs and correcting regimens to slow myopia progression in children is influenced by the extent of the visual field that is manipulated (Smith III, 2013). In particular, the relative treatment effects reported for the different types of optical treatment regimens for myopia are in general agreement with the eccentricity-dependent decrease in efficacy

observed beyond the near periphery in this study. For example, multifocal contact lenses and orthokeratology treatment strategies, which typically produce relative myopic defocus much closer to the fovea than spectacle lens regimens, have typically been shown to be more effective in reducing myopia progression (Sankaridurg, 2017, Smith III, 2013, Wildsoet et al., 2019). Similarly, in comparison to other currently available spectacle lens designs, the Defocus Incorporated Multiple Segments (DIMS) spectacle lens appears to be one of the more effective spectacle lens designs. In this respect, it may be significant that the annular positive powered treatment zones of the DIMs lens begin at eccentricities of about 7°-8° that are well within the effective range of eccentricities noted in Figure 6 (Lam, Tang, Tse, Lee, Chun, Hasegawa, Qi, Hatanaka & To, 2020).

While it is very likely that other optical parameters (e.g., treatment add power) influence the effective range of treatment eccentricities, the results from this investigation indicate that the near periphery has a strong influence on the overall ability of imposed myopic defocus to slow myopia progression. Limiting the imposed defocus to eccentricities beyond the near periphery may have little therapeutic benefit.

Supplementary Material

Refer to Web version on PubMed Central for supplementary material.

Acknowledgement

This work was supported by National Institutes of Health Grants EY-03611 and EY-07551, funds from the Brien Holden Vision Institute, and the University of Houston Foundation.

References

Arumugam B, Hung L-F, To C-H, Holden BA, & Smith EL III (2014). The effects of simultaneous dual focus lenses on refractive development in infant monkeys. Investigative Ophthalmology & Visual Science, 55, 7423–7432. [PubMed: 25324283]

Arumugam B, Hung L-F, To C-H, Sankaridurg P, & Smith EL III (2016). The effects of the relative strength of simultaneous competing defocus signals on emmetropization in infant monkeys. Investigative Ophthalmology & Visual Science, 57, 3949–3960. [PubMed: 27479812]

Barathi VA, Boopathi VG, Yap EPH, & Beuerman RW (2008). Two models of experimental myopia in the mouse. Vision Research, 48, 904–916. [PubMed: 18289630]

Benavente-Perez A, Nour A, & Troilo D (2012). The effect of simultaneous negative and positive defocus on eye growth and development of refractive state in marmosets. Investigative Ophthalmology & Visual Science, 53, 6479–6487. [PubMed: 22918633]

Benavente-Perez A, Nour A, & Troilo D (2014). Axial eye growth and refractive error development can be modified by exposing the peripheral retina to relative myopic and hyperopic defocus. Investigative Ophthalmology & Visual Science, 55, 6765–6773. [PubMed: 25190657]

Bowrey H, Zeng G, Tse DY, Leotta A, Wu Y, To C-H, Wildsoet CF, & McFadden SA (2017). The effect of spectacle lenses containing peripheral defocus on refractive error and horizontal eye shape in guinea pig. Investigative Ophthalmology & Visual Science, 58, 2705–2714. [PubMed: 28549092]

Bullimore MA, & Brennan NA (2019). Myopia control: Why each diopter matters. Optometry and Vision Science, 96, 463–465. [PubMed: 31116165]

Carkeet A (1998). Field restriction and vignetting in contact lenses with opaque peripheries. Clinical and Experimental Optometry, 81, 151–158. [PubMed: 12482252]

Flitcroft DI (2012). The complex interactions of retinal, optical and environmental factors in myopia aetiology. Progress in Retinal Eye Research, 622–660. [PubMed: 22772022]

Harris WF (1988). Algebra of sphero-cylinders and refractive errors, and their means, variance, and standard deviation. American Journal of Optometry and Physiological Optics, 65, 794–902. [PubMed: 3207150]

Hartwig A, Charman WN, & Radhakrishnan H (2011). Accommodative response to peripheral stimuli in myopes and emmetropes. Ophthalmic & Physiological Optics, 31, 91–99. [PubMed: 21054470]

Holden BA, Fricke TR, Wilson DA, Jong M, Naidoo KS, Sankaridurg P, Wong TY, Naduvilath T, & Resnikoff S (2016). global prevalence of myopia and high myopia and tempral trens from 2000 to 2050. Ophthalmology, 123, 1036–1042. [PubMed: 26875007]

Howlett MH, & McFadden SA (2009). Spectacle lens compensation in the pigmented guinea pig. Vision Research, 49, 219–227. [PubMed: 18992765]

Hung L-F, Crawford MLJ, & Smith EL III (1995). Spectacle lenses alter eye growth and the refractive status of young monkeys. Nature Medicine, 1, 761–765.

Irving EL, Callender MG, & Sivak JG (1995). Inducing ametropias in hatchling chicks by defocus -- apperture effects and cylindrical lenses. Vision Research, 35, 1165–1174. [PubMed: 7610578]

Kee C.-s., Hung L-F, Qiao-Grider Y, Roorda A, & Smith EL III (2004). Effects of optically imposed astigmatism on emmetropization in infant monkeys. Investigative Ophthalmology & Visual Science, 45, 1647–1659. [PubMed: 15161822]

Kee C. s., Hung L-F, Qiao Y, & Smith EL III (2003). Astigmatism in infant monkeys reared with cylindrical lenses. Vision Research, 43, 2721–2739. [PubMed: 14568091]

Labhishetty V, Cholewiak SA, & Banks MS (2019). Contributions of foveal and non-foveal retina to the human eye's focusing response. Journal of Vision, 19, 1–15.

Lam CSY, Tang WC, Tse DY, Lee RPK, Chun RKM, Hasegawa K, Qi H, Hatanaka T, & To C-H (2020). Defocus Incorporated Multiple Segments (DIMS) spectacle lenses to slow myopia progression : a 2-year randomised clinical trial. British Journal of Ophthalmology, 104, 363–368.

Liu Y, & Wildsoet CF (2011). The effect of 2-zone concentric bifocal spectacle lenses on refractive error development and eye growth in young chicks. Investigative Ophthalmology & Visual Science, 52, 1078–1086. [PubMed: 20861487]

Liu Y, & Wildsoet CF (2012). The effective add inherent in 2-zone negative lenses inhibits eye growth in myopic young chicks. Investigative Ophthalmology & Visual Science, 53, 5085–5093. [PubMed: 22761258]

Maier FM, Howland HC, Ohlendorf A, Wahl S, & Schaeffel F (2015). Lack of oblique astigmatism in the chicken eye. Vision Research, 109, 68–76. [PubMed: 25701740]

McFadden SA, Tse DY, Bowrey HE, Leotta AJ, Lam CS, Wildsoet CF, & To C-H (2014). Integratioin of defocus by dual power Fresnel lenses inhibits myopia in the mammalian eye. Investigative Ophthalmology & Visual Science, 55, 908–917. [PubMed: 24398103]

Norton TT, & Rada JA (1995). Reduced extracellualar matrix accumulation in mammalian sclera with induced myopia. Vision Research, 35, 1271–1281. [PubMed: 7610587]

Norton TT, & Siegwart JT (1995). Animal models of emmetropization: matching axial length to the focal plane. Journal of the American Optometric Association, 66, 405–414. [PubMed: 7560727]

Rada JA, Nickla DL, & Troilo D (2000). Decreased proteoglycan synthesis associated with form deprivation myopia in mature primate eyes. Investigative Ophthalmology & Visual Science, 41, 2050–2058. [PubMed: 10892842]

Rolls ET, & Cowey A (1970). Topography of the retina and striate cortex and its relationship to visual acuity in rhesus monkeys and squirrel monkeys. Experimental Brain Research, 10, 298–310. [PubMed: 4986000]

Sankaridurg P (2017). Contact lenses to slow progression of myopia. Clinical and Experimental Optometry, 100, 432–437. [PubMed: 28752898]

Schaeffel F (2017). Biologische mechanismen der myopie. Ophthalmologe, 114, 5–19. [PubMed: 27837267]

Schaeffel F, Glasser A, & Howland HC (1988). Accommodation, refractive error and eye growth in chickens. Vision Research, 28, 639–657. [PubMed: 3195068]

Smith EL III (2011). Charles F. Prentice Award Lecture 2010: A case for peripheral optical treatment strategies for myopia. Optometry and Vision Science, 88, 1029–1044. [PubMed: 21747306]

Smith EL III (2013). Optical treatment strategies to slow myopia progression: Effects of the visual extent of the optical treatment zone. Experimental Eye Research, 114, 77–88. [PubMed: 23290590]

Smith EL III, & Hung L-F (1999). The role of optical defocus in regulating refractive development in infant monkeys. Vision Research, 39, 1415–1435. [PubMed: 10343811]

Smith EL III, Hung L-F, & Huang J (2009). Relative peripheral hyperopic defocus alters central refractive development in monkeys. Vision Research, 49, 2386–2392. [PubMed: 19632261]

Smith EL III, Hung L-F, & Huang J (2012). Protective effects of high ambient lighting on the development of form-deprivation myopia in rhesus monkeys. Investigative Ophthalmology & Visual Science, 53, 421–428. [PubMed: 22169102]

Smith EL III, Hung L-F, Huang J, & Arumugam B (2013). Effects of local myopic defocus on refractive development in monkeys. Optometry and Vision Science, 90, 1176–0086. [PubMed: 24061154]

Smith EL III, Kee C.-s., Ramamirtham R, Qiao-Grider Y, & Hung L-F (2005). Peripheral vision can influence eye growth and refractive development in infant monkeys. Investigative Ophthalmology & Visual Science, 46, 3965–3972. [PubMed: 16249469]

Smith EL III, Ramamirtham R, Qiao-Grider Y, Hung L-F, Huang J, Kee C.-s., Coats D, & Paysee E (2007). Effects of foveal ablation on emmetropization and form-deprivation myopia. Investigative Ophthalmology & Visual Science, 48, 3914–3922. [PubMed: 17724167]

Troilo D, Smith ELI, Nickla DL, Ashby R, Tkatchenko AV, Ostrin L, Gawne TJ, Pardue MT, Summers JA, Kee C.-s., Schroedl F, Wahl S, & Jones L (2019). IMI - Report on Experimental Models of Emmetropization and Myopia. Investigative Ophthalmology & Visual Science, 60 (Special Issue No. 3), 31–88.

Tse DY, Lam CS, Guggenheim JA, Lam C, Li K-K, Liu Q, & To C-H (2007). Simultaneous defocus integration during refractive development. Investigative Ophthalmology & Visual Science, 48, 5352–5359. [PubMed: 18055781]

Wallman J, & Winawer J (2004). Homeostasis of eye growth and the question of myopia. Neuron, 43, 447–468. [PubMed: 15312645]

Whatham A, & Judge S (2001). Compensatory changes in eye growth and refraction induced by daily wear of soft contact lenses in young marmosets. Vision Research, 41, 267–273. [PubMed: 11164443]

Wildsoet CF, Chia A, Cho P, Guggenheim JA, Polling JR, Read SA, Sankaridurg P, Saw SM, Trier K, Walline JJ, Wu PC, & Wolffsohn JS (2019). IMI - Interventions for controling myopia onset and progression report. Investigative Ophthalmology & Visual Science, 60, M106–M131. [PubMed: 30817829]

Wong TY, Ferreira A, Hughes R, Carter G, & Mitchel P (2014). Epidemiology and disease burden of pathologic myopia and myopic choroidal neovascularization: An evidence-based systematic review. American Journal of Ophthalmology, 157, 9–25. [PubMed: 24099276]

Zhu X, Winawer JA, & Wallman J (2003). Potency of myopic defocus in spectacle lens compensation. Investigative Ophthalmology & Visual Science, 44, 2818–2827. [PubMed: 12824218]

Highlights

- In response to competing defocus signals emmetropization targets the more myopic focus
- Peripheral myopic defocus can slow axial growth and produce hyperopia in monkeys
- The effects of myopic defocus on refractive development decrease with eccentricity
- Treatment strategies for myopia should impose myopic defocus in the near periphery

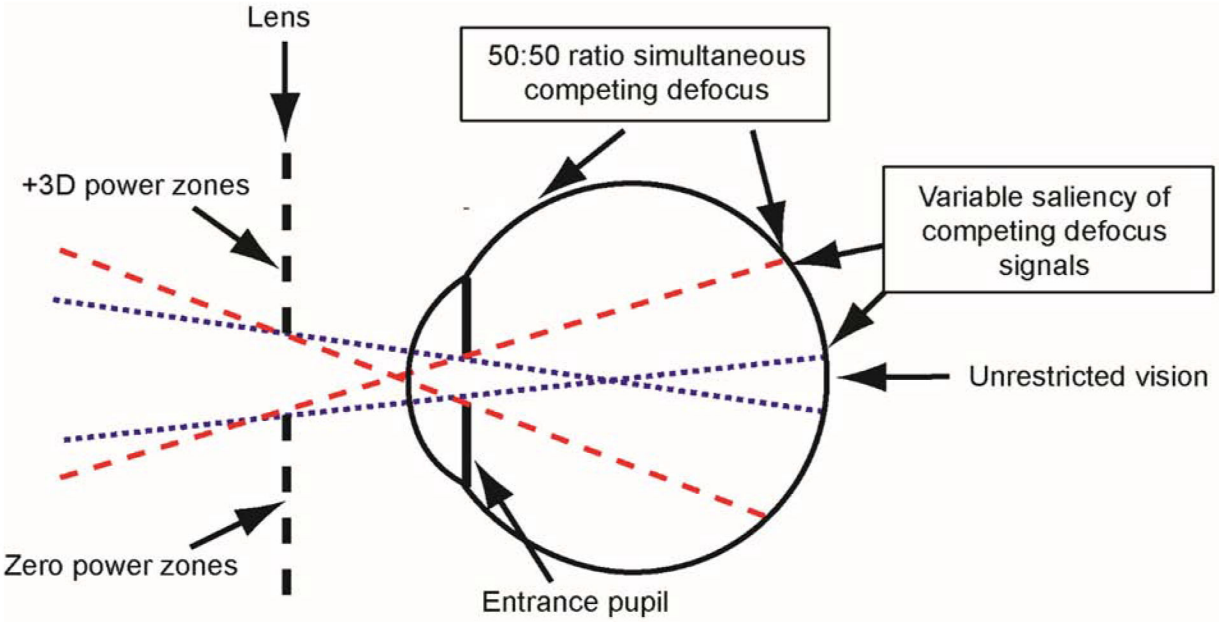

Figure 1.

Schematic diagram of the extent of the visual field influenced by the different power zones of the dual-focus lenses. The blue dotted lines represent the projection of the eye's entrance pupil through the central, zero-power zone and delineate the object locations that are imaged exclusively through the central zone (i.e., unrestricted portion of the visual field). The red dashed lines delineate the object eccentricities beyond which all objects are imaged exclusively through the dual-powered portion of the lens, resulting in images that are formed simultaneously at two different focal planes. These image planes have approximately equal amounts of light refracted through the plano and +3D components of the lens. For objects between the blue and red projection lines, the resulting images are also formed at two competing image planes, with the proportion of rays entering through the central lens zone decreasing with eccentricity while those entering through the dual-focus segments increase. See the Supplementary materials.

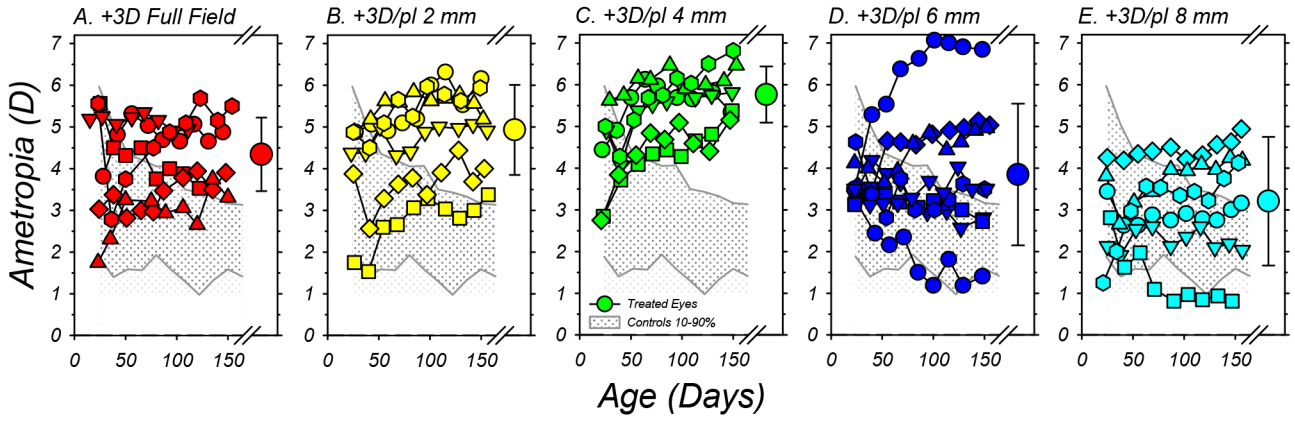

Figure 2.

Spherical-equivalent, spectacle-plane refractions plotted as a function of age for individual subjects reared with the binocular +3D full-field lenses (A) and +3D/pl dual-focus lenses with 2mm (B), 4mm (C), 6mm (D) and 8mm (E) central zone of unrestricted vision. Each of the smaller symbols represents the average ametropia for the left and right eyes of a given animal. The large symbols to the right in each plot show the group average (±SD) at the end of the treatment period. The shaded area in each plot illustrates the 10% to 90% range of ametropias for the normal control animals.

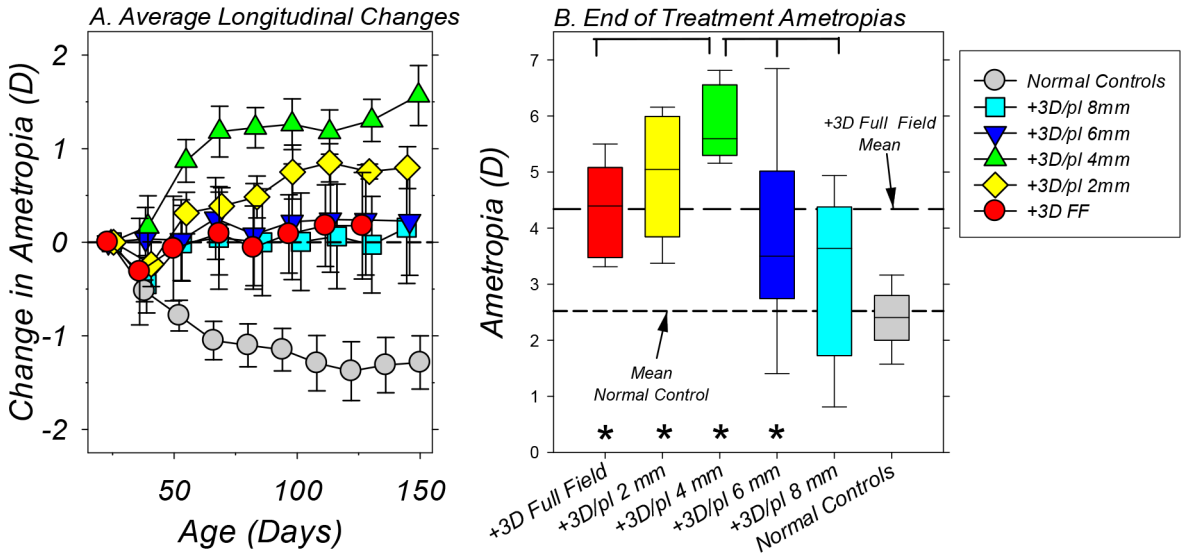

Figure 3.

A. Average (±SEM) binocular change in refractive error from baseline values plotted as a function of age for each subject group. The symbol legend in the figure indicates the color/shading for the different groups. The first symbols in each function represent the start of treatment. B. Box plots of the refractive errors obtained at the end of the lens-rearing period for each treatment group. The horizontal line in each box represents the group median; the lower and upper box boundaries indicate the 25% and 75% limits, respectively; and the lower and upper error bars show the 10% and 90% limits, respectively. The long and short dashed lines represent the mean ametropias for the +3D FF controls and the normal monkeys, respectively, at ages corresponding to the end of the treatment period. The asterisks indicate treated-group refractive errors that were significantly different from that for the normal control monkeys. The horizontal brackets indicate significant differences in the average refractive errors between the 4mm treatment group and other lens-reared groups.

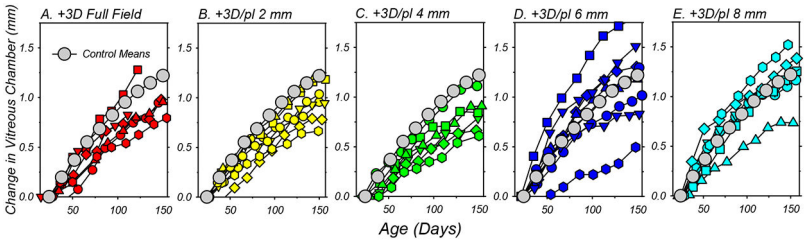

Figure 4.

Binocular average change in vitreous chamber depth from baseline values plotted as a function of age for individual subjects reared with the +3D full-field lenses (A) and +3D/pl dual-focus lenses with 2mm (B), 4mm (C), 6mm (D) and 8mm (E) central zones of unrestricted vision. Each symbol represents the average change in vitreous chamber depth for the left and right eyes of a given animal. The grey symbols in each plot represent the mean changes for the normal control animals.

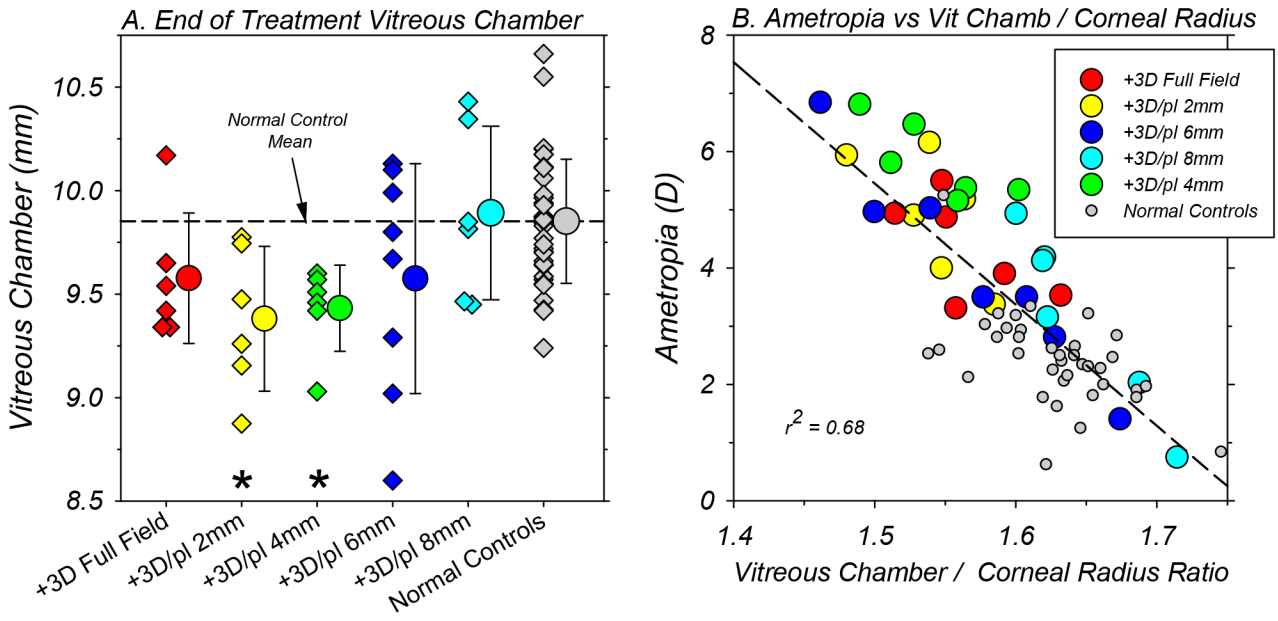

Figure 5.

A. Binocular vitreous chamber depth for individual animals (diamond symbols) in each subject group obtained at ages corresponding to the end of the lens-rearing period. Each of the smaller symbols represents the average vitreous chamber depth for the left and right eyes of a given animal. The larger circular symbols next to the individual data represent the group means (±SD). The asterisks indicate mean values that were significantly different from that for the normal control monkeys. B. Refractive errors (right and left eye averages) obtained at ages corresponding to the end of the treatment period for individual animals plotted as a function of the ratio of vitreous chamber depth in mm to corneal radius in mm. The color shading for the symbols representing the different treatment groups is shown in the included symbol legend.

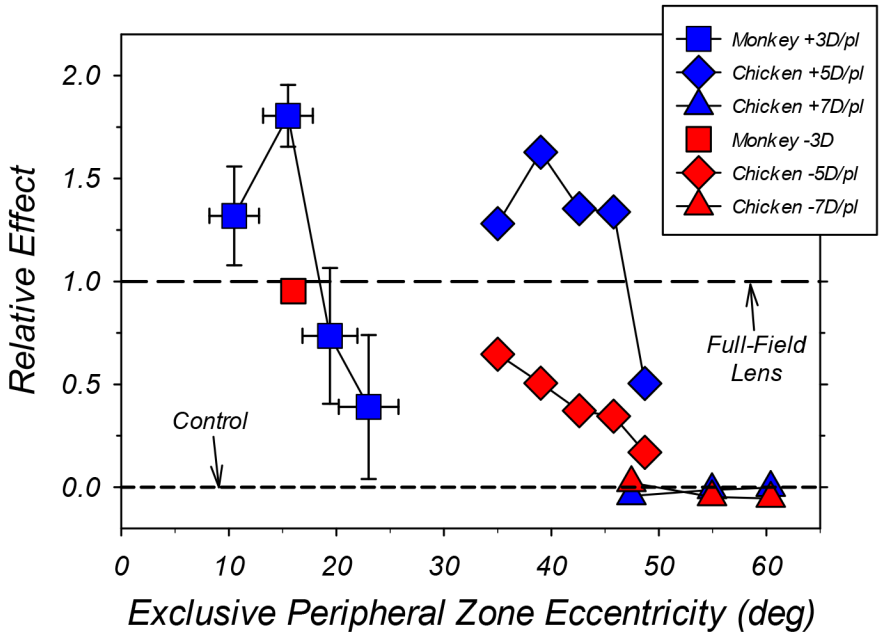

Figure 6.

Comparisons of the average relative effects of the eccentricity of optically imposed defocus on central refractive development for monkeys (square symbols) and chickens (diamond and triangle symbols). In all cases, the bifocal/dual-focus treatment lenses had central zones that provided unrestricted vision and concentric peripheral zones that imposed either myopic (blue symbols) or hyperopic defocus (red symbols). The effect of a given treatment lens is shown relative to the normalized alterations in central refractive error produced by a single-vision treatment lens that had the same power as the peripheral zone of the bifocal/dual-focus lenses. A relative effect of 1.0 indicates that the multifocal treatment lenses produced the same alterations in refractive error as full-field single-vision lenses with powers equal to that of the peripheral zone of the bifocal/dual-focus lenses. Data points plotted above the horizontal line at 1.0 indicate that the bifocal/dual-focus lenses produced larger alterations in refractive development than full-field lenses. The horizontal dashed line at 0.0 indicates that the treatment lenses had no effect on refractive development relative to age-matched controls. The abscissa represents the object eccentricities beyond which all objects were imaged exclusively through the peripheral power zones of the treatment lenses. The vertical error bars for the dual-focus, lens-reared monkeys (blue squares) represent ±1 SEM; the horizontal error bars represent the range in eccentricity associated with a ±1 mm change in vertex distance combined with ±0.6 mm change in entrance pupil size. The data point for imposed peripheral hyperopic defocus (−3.0 D) in monkeys was derived from Smith et al. (2010). The chicken data represented by diamonds and triangles were obtained using peripheral powers of ±5.0 D (Liu and Wildsoet, 2011) *and ±7.0 D (Schippert and Schaeffel, 2006), respectively.*

Table 1.

Refractive errors (median and average ± SD) and other ocular parameters (average ± SD) at the end of the lens-rearing period for all of the subject groups. For a given animal, the right and left eye data were averaged. The asterisks indicate parameters that were significantly different from those for age-matched normal control monkeys. Hashtags indicate significant differences between the +3D/pl 4mm group and other lens-reared groups.

Group	Refractive Error (D) Median Average ± SD	Corneal Power (D)	Anterior Chamber Depth (mm)	Lens Thickness (mm)	Vitreous Chamber Depth (mm)
Normal Controls	+2.50 +2.52 ± 1.00	55.93 ± 1.60	3.09 ± 0.29	3.62 ± 0.21	9.84 ± 0.31
+3 D Full-Field	+4.39* +4.34 ± 0.88#	55.08 ± 0.69	2.90 ± 0.13*	3.56 ± 0.16	9.59 ± 0.32
+3D/pl 2mm	+5.19* +5.08 ± 0.94	55.45 ± 1.00	3.06 ± 0.08	3.67 ± 0.15	9.38 ± 0.35*
+3D/pl 4mm	+5.59* +5.83 ± 0.67	55.39 ± 1.09	3.05 ± 0.14	3.65 ± 0.15	9.40 ± 0.23*
+3D/pl 6mm	+3.50* +3.85 ± 1.70#	55.72 ± 1.63	2.99 ± 0.19	3.68 ± 0.12	9.57 ± 0.55
+3D/pl 8mm	+3.64 +3.21 ± 1.54#	56.86 ± 1.75	2.98 ± 0.13	3.73 ± 0.12	9.90 ± 0.42#